

Binding studies of the anti-retroviral drug, efavirenz to calf thymus DNA using spectroscopic and voltammetric techniques

Marzieh Sadeghi,^{a*} Maryam Bayat,^a Shekofeh Cheraghi,^a Khirollah Yari,^b Rouhollah Heydari,^c Sara Dehdashtian^a and Mojtaba Shamsipur^a

ABSTRACT: Interactions between efavirenz (EFZ) with calf thymus DNA (CT-DNA) were investigated *in vitro* under stimulated physiological conditions using multispectroscopic techniques, cyclic voltammetry viscosity measurement, and gel electrophoresis. Methylene blue and acridine orange dyes were used as spectral probes by fluorescence spectroscopy. Hypochromicity was observed in ultra-violet (UV) absorption band of EFZ. Considerable fluorescence enhancement of EFZ was observed in the presence of increasing amounts of DNA solution and the binding constants (K_b) and corresponding numbers of binding sites (n) were calculated at different temperatures. Thermodynamic parameters including enthalpy change (ΔH) and entropy change (ΔS) were calculated to be $-304.78 \text{ kJ mol}^{-1}$ and $-924.52 \text{ J mol}^{-1} \text{ K}^{-1}$ according to the van 't Hoff equation, which indicated that reaction is predominantly enthalpically driven. In addition, UV/vis absorption titration of DNA bases confirmed that EFZ interacted with guanine and cytosine preferentially. Gel electrophoresis of DNA with EFZ demonstrated that EFZ also has the ability to cleave supercoiled plasmid DNA. Circular dichroism study showed stabilization of the right-handed B form of CT-DNA. All results suggest that EFZ interacts with CT-DNA via an intercalative mode of binding. Copyright © 2015 John Wiley & Sons, Ltd.

RESEARCH HIGHLIGHTS:

- The interaction of efavirenz as an anticancer and anti-retroviral drug with calf thymus DNA (CT-DNA) was studied using multispectroscopic methods combined with cyclic voltammetry.
- Hydrogen bonds and van der Waals forces play main roles in the binding of efavirenz to CT-DNA.
- The drug interacted with DNA in an intercalating mode with a binding constant of $3.50 (\pm 0.06) \times 10^4 \text{ mol}^{-1} \text{ L}$.

Keywords: efavirenz; dna interaction; intercalation

Introduction

Efavirenz (EFZ), (S)-6-chloro-4(cyclopropylethynyl)-1,4-dihydro-4-(trifluoromethyl)-2H-3,1-benzoxazin-2-one (Fig. 1), is an anti-human immunodeficiency virus (anti-HIV) agent. EFZ is a non-nucleoside reverse-transcriptase inhibitor (NNRTI) used in the treatment of patients with HIV infection (1). EFZ is used in combination with either protease inhibitors (PIs) or nucleoside reverse-transcriptase inhibitors (NRTIs) (2). NNRTIs of HIV-1 have recently received a lot of attention. These drugs stop HIV from multiplying by preventing the RT enzyme from working. This enzyme transcribes HIV genetic material (single-stranded RNA) into double-stranded DNA. This step has to occur before the HIV genetic code gets inserted into the genetic code of an infected cell. EFZ is also used in combination with other anti-retroviral agents as part of an expanded post-exposure prophylaxis regimen to reduce the hazard of HIV infection in people exposed to a significant risk (e.g. needlestick injuries, certain types of unprotected sex etc.). Current guidelines for the management of HIV patients suggest the use of two NRTIs, such as lamivudine and zidovudine, in combination with a NNRTI, such as EFZ (3).

DNA is an important genetic substance of life that carries most of the hereditary information and facilitates the biological synthesis of proteins and enzymes through the replication and

transcription of this information (4). DNA has been defined as a primary target molecule for most anti-cancer and anti-viral therapies according to cell biologists. Therefore, investigations of interactions of DNA with small molecules are vital for the design of new types of pharmaceutical molecules (5,6). It is well known that small molecules can interact with the DNA double helix through three dominant modes (7): first, intercalative binding, in which the molecules intercalate within the DNA base pairs, which would distort the DNA

* Correspondence to: M. Sadeghi, Department of Chemistry, Razi University, Kermanshah, Iran. E-mail: m.sadeghi@razi.ac.ir or negarsade@gmail.com

^a Department of Chemistry, Razi University, Kermanshah, Iran

^b Medical Biology Research Center, Kermanshah University of Medical Science, Kermanshah, Iran

^c Razi Herbal, Medicines Research Center, Lorestan University of Medical Sciences, P.O. Box 68149-89468, Khorramabad, Iran

Abbreviations: AO, acridine orange; CV, cyclic voltammetric; HIV, human immunodeficiency virus; MB, methylene blue; NNRTI, non-nucleoside reverse-transcriptase inhibitor; NRTI, nucleoside reverse-transcriptase inhibitor; PI, protease inhibitors; RT, reverse transcriptase; UV, ultra-violet.

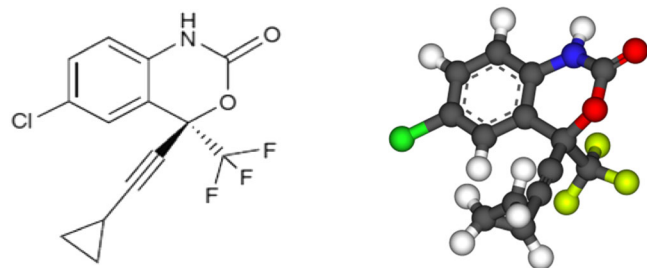


Figure 1. Molecular (left) and stereographic (right) structure of efavirenz.

strands by unwinding of the double helix; second, electrostatic binding between the negatively charged DNA phosphate backbone and cationic or positive end of the molecules; and third, groove binding involving van der Waal's interactions in the deep major groove or the shallow minor groove of the DNA helix, which prevent DNA replication to defend against disease (8,9).

One approach to accelerate the availability of new drugs is to reposition drugs approved for other indications as anti-cancer agents (10,11). Recently, Sahabadi *et al.* reported the interaction of some anti-viral drugs with DNA (10–12). In this context, we studied the interaction of the anti-viral drug, EFZ (Fig. 1) with calf thymus DNA. In this work, the *in vitro* interaction between EFZ and calf thymus DNA (CT-DNA) was investigated under simulated physiological conditions using UV-vis absorption, fluorescence and circular dichroism (CD) spectroscopy, cyclic voltammetry, as well as DNA melting temperature and viscosity measurements. Acridine orange (AO) and methylene blue (MB) as DNA probes were used for a comparative study of the binding affinity of EFZ to the DNA helix, and its interaction mechanisms were also discussed. The drug binding mode and thermodynamic characteristic were explored. Interaction of EFZ with plasmid circular DNA (pUC18) employing gel electrophoresis was also demonstrated.

The results provide useful insights into drug–DNA interactions, which are valuable for the rational design of drugs that are more efficient as well as understanding the binding mechanism of these drugs with specific DNA sequences.

Experimental

Materials and methods

Highly polymerized CT-DNA, EFZ, AO and HEPES were purchased from Sigma. DNA bases [adenine (A), thymine (T), guanine (G) and cytosine (C)], AO and MB were purchased from Merck. All solutions were prepared using deionized Milli-Q water. HEPES buffer solution was prepared from 4-(2-hydroxyethyl)-1-piperazineethanesulfonic acid and the pH was adjusted to 7.4. The stock solution of DNA was prepared by dissolving DNA in 0.05 mol L^{-1} of the HEPES buffer at pH 7.4. The concentration of DNA solution was expressed in monomer units, which were determined by spectrophotometry at 260 nm using an extinction coefficient (ϵ_p) of $6600 \text{ mol}^{-1} \text{ L cm}^{-1}$ (13). The stock solution was stored at 4°C . A solution of DNA gave a ratio of UV absorbance at 260 and 280 nm, A_{260} / A_{280} more than 1.8, indicating that DNA was sufficiently free from protein (14). MB and AO dye stock solutions ($1.0 \times 10^{-4} \text{ mol L}^{-1}$) were prepared by dissolving in HEPES (pH 7.4) buffer and diluting to their required volume. An EFZ stock solution ($1.0 \times 10^{-3} \text{ mol L}^{-1}$) was prepared daily by dissolving an appropriate amount of compound in HEPES buffer.

Instrumentation

The UV-vis spectra for DNA–EFZ interactions were obtained using an Agilent 8453 spectrophotometer. Solutions of DNA and EFZ were scanned in a 1-cm quartz cuvette. Absorbance experiments were carried out by keeping the concentration of EFZ constant ($5.0 \times 10^{-5} \text{ mol L}^{-1}$) while varying the DNA concentration from 0 to $1.5 \times 10^{-4} \text{ mol L}^{-1}$. Absorbance values were recorded after each successive addition of DNA solution and equilibration. Our experiments for determining the melting temperature were carried out for CT-DNA in the absence and presence of different amounts of drug. The melting plot of DNA ($5.0 \times 10^{-5} \text{ mol L}^{-1}$) was monitored by plotting the UV maximum absorption of DNA at 260 nm versus temperature.

Fluorescence intensities were measured using a JASCO spectrofluorimeter (FP 6200) by keeping the concentration of drug constant while varying the DNA concentration from 0.0 to $14 \times 10^{-5} \text{ mol L}^{-1}$ at three different temperatures (298, 303, or 310 K). In the competitive binding studies, the fluorescence spectra of DNA–AO and DNA–MB complex and the mixture of different concentrations of EFZ to DNA–AO and DNA–MB complex were measured under pH 7.4 HEPES buffer, respectively.

Iodide quenching experiments were conducted by adding stoichiometric small aliquots of potassium iodide stock solution (0.01 mol L^{-1}) to EFZ and EFZ–DNA complex solutions, respectively. The fluorescence intensity was recorded, and then the quenching constants were calculated (6)

CD measurements were recorded on a JASCO (J-810) spectropolarimeter, keeping the concentration of DNA constant ($5.0 \times 10^{-5} \text{ mol L}^{-1}$) while varying the concentration of EFZ.

Viscosity measurements were made using a SCHOT viscosimeter (AVS 450), which thermostated at $25 \pm 0.5^\circ\text{C}$ by a constant temperature bath. The DNA concentration was fixed at $5.0 \times 10^{-5} \text{ mol L}^{-1}$ and flow time was measured with a digital stop watch; the relative viscosities of DNA in the presence and absence of EFZ were calculated from the following eqn (1): (15,16)

$$\frac{\eta}{\eta_0} = \left(\frac{t - t_0}{t_{\text{DNA}} - t_0} \right) \quad (1)$$

where t_0 and t_{DNA} are the observed flow times of the solvent and DNA, respectively, while t is the flow times of the EFZ and DNA mixture. Data are presented as $(\eta/\eta_0)^{1/3}$ versus binding ratio ($[\text{EFZ}]/[\text{DNA}]$), where η is the viscosity of DNA in the presence of EFZ and η_0 is the viscosity of DNA in the absence of EFZ.

Cyclic voltammetric (CV) experiments were performed using the μ -Autolab electrochemical system (Eco-Chemie, Utrecht, The Netherlands) equipped with GPES/FRA 4.9 software coupled with a conventional three-electrode cell. The working electrode was a glassy carbon disc (1.8 mm diameter), the auxiliary electrode was a platinum wire and the reference electrode was a saturated calomel electrode (SCE) (all electrodes were from AZAR Electrode). The surface of the working electrode was polished using a 0.05-mm alumina prior to each experiment and was rinsed with double-distilled water before usage. All experiments were carried out at ambient temperature.

For the gel electrophoresis experiments, Eppendorf microtubes containing mixtures of equal concentrations of pUC18 plasmid DNA and drug samples in Tris–acetate–EDTA (TAE) buffer (pH 8) ($[\text{EFZ}]/[\text{DNA}] = 0.0, 0.5, 1, 1.5$) were incubated in 37°C for 1 h. After this period, 12 μL of the resulting mixture were electrophoresed on a 1% agarose gel containing ethidium bromide (EB). The bands

on the gel were detected by EB fluorescence (at 366 nm) with gel documentation (Quantum ST4).

Results and discussion

DNA-binding mode and affinity

UV-vis spectroscopic studies. UV-vis absorption measurement is an effective method to detect the binding strength and the mode of drug binding with CT-DNA. Binding of EFZ to CT-DNA was studied by the electronic absorption spectral technique. The UV absorption spectra of EFZ were recorded in the absence and presence of DNA. In the ultraviolet region from 220 to 350 nm, EFZ had a strong absorption peak at 247 nm and a weak peak at 300 nm. In the presence of increasing concentrations of CT-DNA, a hypochromic shift by a slight red shift (3 nm) at 247 nm is observed (Fig. 2a). Figure 2(b) shows that the total absorption of free EFZ and free DNA was greater than the absorption of the EFZ–DNA complex. This result reveals a hypochromism effect that occurred after the interaction of EFZ with DNA. At about 247 nm, the hypochromicity reaches as high as about 30% with a minor bathochromic effect (3 nm). This observation gives good evidence of the intercalation of EFZ through the stacking and interaction of the aromatic rings of the drug and the base pairs of DNA (14,17).

In order to further investigate the intensity of the interaction between EFZ and CT-DNA, the intrinsic binding constant, K_b , was calculated from a plot of $[DNA]/(\epsilon_a - \epsilon_f)$ versus $[DNA]$ using eqn (2), (18,19) (Fig. 2a):

$$[DNA]/(\epsilon_a - \epsilon_f) = [DNA]/(\epsilon_b - \epsilon_f) + 1/K_b(\epsilon_b - \epsilon_f) \quad (2)$$

where $[DNA]$ is the concentration of DNA, the molar absorption coefficients ϵ_a , ϵ_b and ϵ_f represent the apparent absorption coefficient for the EFZ, the extinction coefficient for the EFZ in the fully bound form and the extinction coefficient for the free EFZ, respectively. In particular, ϵ_f was determined by a calibration curve of the isolated EFZ in an aqueous solution, following Beer's law. The apparent extinction coefficient, ϵ_a , was determined as the ratio between the observed absorbance (A_{obs}) and the drug concentration, $A_{obs}/[EFZ]$. K_b is given by the ratio of slope to the intercept.

The K_b value obtained was $(3.5 \pm 0.06) \times 10^4 \text{ mol}^{-1} \text{ L}$. This value indicates a high affinity of the complex for binding to DNA. It is comparable with binding constants of well known intercalating agents such as MB ($2.13 \times 10^4 \text{ mol}^{-1} \text{ L}$) and AO ($2.69 \times 10^4 \text{ mol}^{-1} \text{ L}$) (14), it seems that EFZ binds strongly to CT-DNA via an intercalation mechanism.

Thermal denaturation (T_m) studies

Interaction of small molecules with double-stranded DNA can influence the melting temperature (T_m), at which the double helix denatures into single-stranded DNA. Thermal denaturation of DNA is a straight forward method to determine the stabilization/destabilization effect of ligands on DNA double helix. The extent of this stabilization also provides a semi-quantitative evaluation of ligand affinity toward DNA duplex (20). On the other hand, the melting of DNA can be used to distinguish between the molecules that induce intercalation and those that bind externally to the biopolymer, respectively. Intercalation of small molecules into the double helix is known to increase the helix melting temperature stabilizing the natural structure of DNA, while the non-intercalative binding causes no obvious variation upon T_m (21). Our experiments were carried out for CT-DNA in the absence and presence of different amounts of EFZ. The melting plot of DNA ($5.0 \times 10^{-5} \text{ mol L}^{-1}$) was monitored by plotting the UV maximum absorption of DNA at 260 nm versus temperature at various binding ratios (Fig. 3). In the present case, melting temperature (T_m) of DNA in the absence of any added drug has been found to be $70 \pm 0.5^\circ\text{C}$. An increase in the DNA melting temperature by 5 and 6°C , for the above-mentioned concentrations were observed. These values clearly show that the EFZ is able to stabilize DNA helix.

Fluorescence spectroscopic studies

The fluorescence titration experiment has been widely used to characterize the interaction of different drugs with DNA, by following the changes in fluorescence intensity of the drugs. The interactions between the drugs and DNA can prevent the fluorescence emission of the complexes from being quenched by polar solvent molecules and result in the enhancement of fluorescence intensity (22,23).

In the present study, it has been used to monitor the interaction of anti-viral drug EFZ with CT-DNA, and the results were shown in Fig. 4. Under our experimental conditions, an aqueous solution of EFZ exhibits broad fluorescence between 360 and 600 nm with the maximum at around 405 nm when excited at 270 nm.

The fluorescence spectrum of EFZ was markedly affected by the addition of DNA. The emission intensity of EFZ in the presence of DNA is 2 times greater than that in the absence of DNA, with a $[DNA]/[EFZ]$ ratio of two and a red shift of 7 nm. The increase in emission intensity implies that EFZ can insert itself between DNA base pairs. The red shift shows that the EFZ is protected from solvent water molecules by the hydrophobic environment inside the

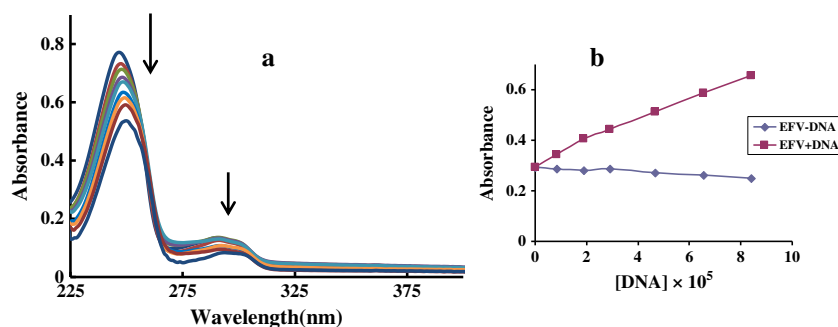


Figure 2. (a) Absorption spectra of EFZ ($5.0 \times 10^{-5} \text{ M}$) in the absence and presence of increasing amounts of DNA, c (DNA) ($\times 10^5 \text{ mol L}^{-1}$: 0.00, 0.75, 1.75, 2.75, 4.50, 6.50, 7.50, 10.00, 15.00) and 298 K. (b) Comparison of absorption between the DNA–EFZ complex and the sum of values for DNA and EFZ at λ_{260} .

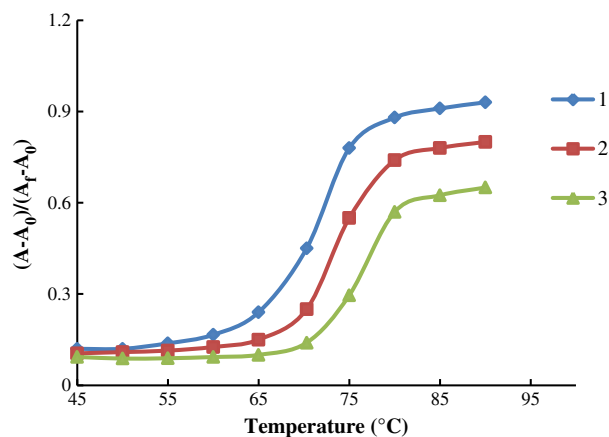


Figure 3. Melting curves of CT-DNA ($5.0 \times 10^{-5} \text{ mol L}^{-1}$) at 260 nm in the absence and the presence of various concentrations of EFZ in HEPES buffer, c (EFZ) ($\times 10^5 \text{ mol L}^{-1}$): 0.00, 2.50, 5.00, where A_0 , A_f and A are the absorbance intensities at 40, 90°C and at a given temperature between 45 and 90°C, respectively.

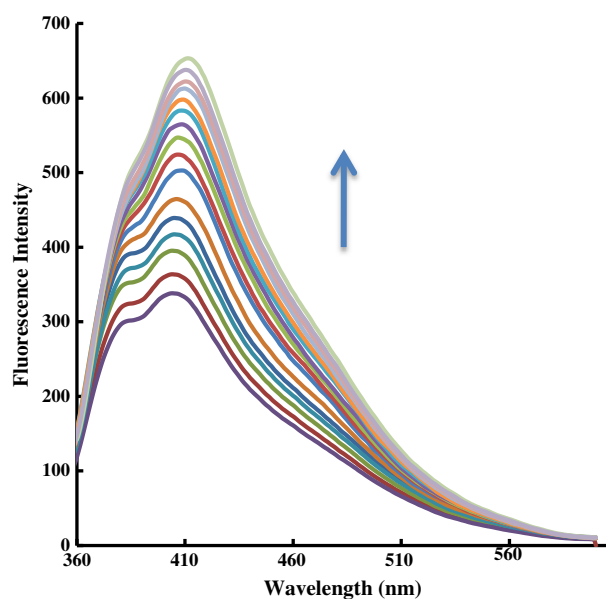


Figure 4. Fluorescence spectra of the EFZ ($5.0 \times 10^{-5} \text{ mol L}^{-1}$) in the absence and presence of increasing amounts of DNA c (DNA) ($\times 10^5 \text{ mol L}^{-1}$): 0.00, 0.50, 1.50, 2.25, 2.75, 4.00, 5.00, 6.25, 6.75, 8.00, 9.25, 10.00, 11.75, 13.75, 15.00 and 310 K.

DNA helix (6,12,23,24). This marked increase in emission intensity also agrees with findings obtained with other intercalators (25).

Analogous to the quenching constant in a quenching process, the enhancement constant can be obtained from the following equation (12,13):

$$\frac{F_0}{F} = 1 - K_D [E] \quad (3)$$

If a dynamic process is a part of the enhancing mechanism, the above equation can be written as follows (12,26):

$$\frac{F_0}{F} = 1 - K_D [E] = 1 - K_B \tau_0 [E] \quad (4)$$

where K_D is the dynamic enhancement constant (like a dynamic quenching constant), K_B is the bimolecular enhancement constant

(like a bimolecular quenching constant) and τ_0 is the lifetime of the fluorophore in the absence of the enhancer. The dynamic enhancement constant of EFZ at different temperatures were calculated using eqn (4) (Table 1 and Fig. 5).

Since fluorescence lifetime is typically near 10^{-8} s , the bimolecular enhancement constant (K_B) was calculated from $K_D = K_B \tau_0$ (Table 1). By considering the equivalency of the bimolecular quenching and enhancement constants, it can be seen that the latter constant (K_B) is greater than the largest possible value ($1.0 \times 10^{10} \text{ mol L}^{-1} \text{ sec}^{-1}$) in aqueous medium(12,27). Thus, the fluorescence enhancement is not initiated by a dynamic process, but is instead due to a static process involving ground state complex formation. The possibility for ground state complex formation is supported by observed changes in the absorption spectra during the titration of the drug with CT-DNA, as shown in Fig. 2. Because dynamic quenching only affects the excited state, no changes are expected in the ground state. Alternatively, a static process only involves complex formation in the ground state (13).

Binding constants and the number of binding sites

Fluorescence titration data were used to determine the binding constant (K_f) and binding stoichiometry (n) for the complex formed between EFZ and CT-DNA. Figure 4 shows the fluorescence spectra of EFZ in the presence of different concentrations of CT-DNA. As can be seen from Fig. 4, the fluorescence intensity was increased in the presence of CT-DNA. This change in fluorescence intensity at 405 nm was used to estimate K_f and n for the binding of EFZ to CT-DNA from the following equation (28):

Table 1. Dynamic enhancement and biomolecular enhancement constants for interactions between EFZ and CT-DNA at different temperatures

Temperature (K)	R^2	K_D	K_B
298	0.99	2270 ± 37	$(2.27 \pm 0.04) \times 10^{11}$
303	0.99	3085 ± 48	$(3.08 \pm 0.05) \times 10^{11}$
310	0.99	3671 ± 82	$(3.67 \pm 0.08) \times 10^{11}$

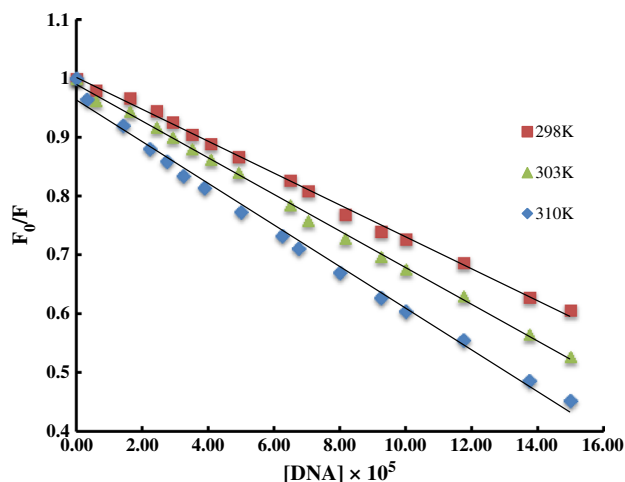


Figure 5. Stern-Volmer plot for observed fluorescence enhancement of EFZ upon addition of DNA at different temperatures.

Table 2. Binding constants (K_f) and number of binding sites (n) of the complex–DNA system at different temperatures

Temperature (K)	R ²	n	K _f	Log K _f
298	0.99	(1.98 ± 0.07)	(1.15 ± 0.36) × 10 ⁵	5.06 ± 0.18
303	0.99	(1.90 ± 0.06)	(2.19 ± 0.10) × 10 ⁴	4.34 ± 0.16
310	0.99	(1.81 ± 0.03)	(1.20 ± 0.09) × 10 ³	3.08 ± 0.05

$$\frac{\log (F_0 - F)}{F} = \log K_f + n \log [DNA] \quad (5)$$

Here F_0 and F are the fluorescence intensities of the fluorophore in the absence and presence of different concentrations of CT-DNA, respectively. In the case of enhanced emission intensity, that is, $F_0 < F$, eqn (5) becomes (12):

$$\frac{\log (F - F_0)}{F} = \log K_f + n \log [DNA] \quad (6)$$

The K_f values and n at different temperatures are given in Table 2. The values of K_f clearly underscore the remarkably high affinity of EFZ to DNA. The size of the binding site makes it possible to distinguish between intercalating and non-intercalating binding agents (12,29). Molecules showing large binding site sizes are indicative of non-intercalative binding mechanisms, which require correspondingly lower concentrations to saturate the sites. Shahabadi and *et al.* (12) reported that the binding of anti-viral drug, valacyclovir to the CT-DNA conforms to an intercalative mechanism with $K_f = 2.7 \times 10^4 \text{ mol}^{-1} \text{ L}$ at 25°C. Our results appear to follow a similar trend. Therefore, the calculated binding site size is again indicative of intercalative binding of EFZ to CT-DNA.

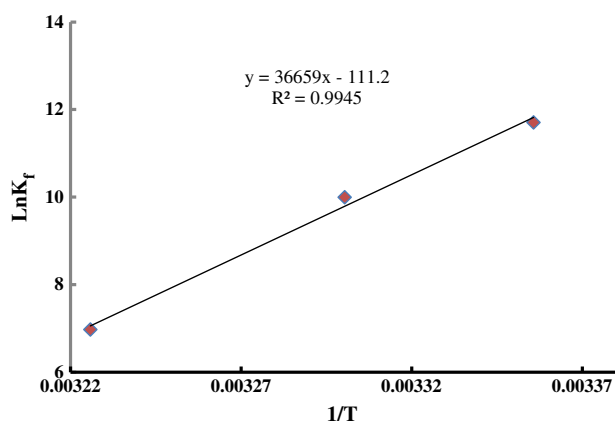


Figure 6. Van 't Hoff plot for the EFZ–DNA complex.

Thermodynamic studies

The interaction forces between drug and biomolecule may involve hydrophobic forces, electrostatic interactions, van der Waals interactions, hydrogen bonds, etc. (30). According to the data of enthalpy changes (ΔH) and entropy changes (ΔS), the model of interaction between drug and biomolecule can be concluded (12,31): (i) $\Delta H > 0$ and $\Delta S > 0$, hydrophobic forces; (ii) $\Delta H < 0$ and $\Delta S < 0$, van der Waals interactions and hydrogen bonds; (iii) $\Delta H < 0$ and $\Delta S > 0$, electrostatic interactions (26). In order to elucidate the interaction of EFZ with DNA, the thermodynamic parameters were calculated. The plot of $\ln K_f$ versus $1/T$ (Fig. 6 and eqn (7)) allows the determination of ΔH and ΔS . If the temperature does not vary significantly, the enthalpy change can be regarded as a constant. Based on the binding constant at different temperatures, the free energy change can be estimated (Table 3 and eqn (8)) by the following equations:

$$\ln k = -\frac{\Delta H}{RT} + \frac{\Delta S}{R} \quad (7)$$

$$\Delta G = \Delta H - T\Delta S \quad (8)$$

where K_f is the binding constant at the corresponding temperature and R is gas constant. It can be seen that the negative value of ΔG revealed that the interaction process is spontaneous; the negative ΔH and ΔS values indicated that hydrogen bonds and van der Waals forces play main roles in the binding of EFZ to DNA. The presence of electronegative elements in EFZ facilitated its interaction with the DNA molecule through hydrogen bonding with the GC and AT hydrogen (1).

Fluorescence competitive binding studies

Competitive binding between AO and EFZ for DNA. In order to obtain an insight into the binding mode between EFZ and DNA, a competitive binding experiment using AO was performed. AO is a classic intercalating dye (7,32,33).

The fluorescence intensity of AO ($3.0 \times 10^{-6} \text{ mol L}^{-1}$) increased after binding with DNA (up to $8.0 \times 10^{-5} \text{ mol L}^{-1}$), but after addition of more DNA the fluorescence intensity was not enhanced further. The effects of EFZ on the fluorescence spectra of DNA–AO systems were measured. It should be noted that the effect of EFZ on the pure AO spectrum has been carefully checked, and no variation in the fluorescence spectrum was detected. Therefore, if EFZ intercalated into the helix of DNA, it would compete with AO for the intercalation

Table 3. Thermodynamic parameters and binding constant for the binding of EFZ to calf thymus DNA ΔG°

Temperature (K)	Ln K _f (mol ⁻¹ L)	ΔG° (kJ mol ⁻¹)	ΔH° (kJ mol ⁻¹)	ΔS° (J mol ⁻¹ K ⁻¹)
298	11.65	−28.99		
303	9.99	−25.17	−304.78 ± 2.60	−924.52 ± 8.90
310	7.09	−17.96		

sites in DNA and lead to a significant decrease in the fluorescence intensity of the AO–DNA complex. By addition of EFZ to the DNA–AO solution, the fluorescence of AO was decreased, suggesting that EFZ could intercalate into the double helix of DNA (Fig. 7).

Competitive binding between MB and EFZ for DNA. In order to provide further evidence for the interaction mode, binding of EFZ to CT-DNA has been studied by a competitive binding fluorescence experiment using MB as a probe. MB is a phenothiazinium dye that can interact with DNA by intercalation, and it has been tested using several spectroscopic methods (34–36).

The results revealed that by addition of CT-DNA, the fluorescence of MB ($5.0 \times 10^{-6} \text{ mol L}^{-1}$) efficiently quenched. MB fluorescence reached minimum after addition of $5.0 \times 10^{-5} \text{ mol L}^{-1}$ DNA; after addition of more DNA the fluorescence spectrum was constant. This emission-quenching phenomenon is due to the changes in the excited-state electronic structure as a consequence of electronic interactions in the MB–DNA complex (34,37).

The effects of EFZ on the fluorescence spectra of DNA–MB systems were measured. As shown in Fig. 8, the fluorescence intensity

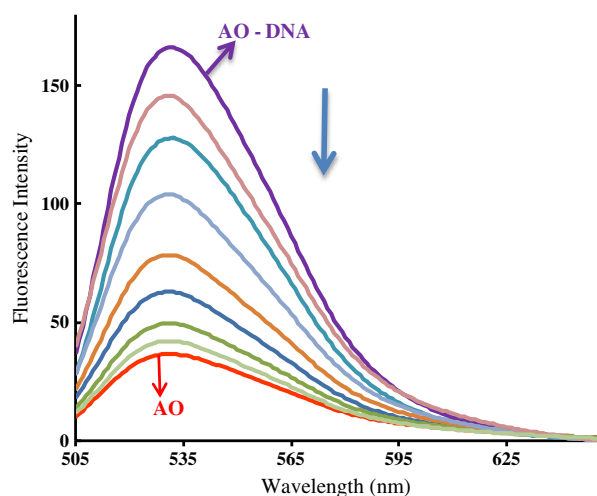


Figure 7. Emission spectra of the AO–DNA complexes on adding various concentration of EFZ, $c(\text{AO}) = 3.0 \times 10^{-6} \text{ mol L}^{-1}$, $c(\text{DNA}) = 8.0 \times 10^{-5} \text{ mol L}^{-1}$, $c(\text{EFZ}) (\times 10^{-5} \text{ mol L}^{-1})$: 0.00, 1.00, 2.00, 3.00, 3.80, 4.80, 6.90, 8.90, 10.00, 12.80, 15.10, 18.00, $\lambda_{\text{ex}} = 490 \text{ nm}$ at 310 K.

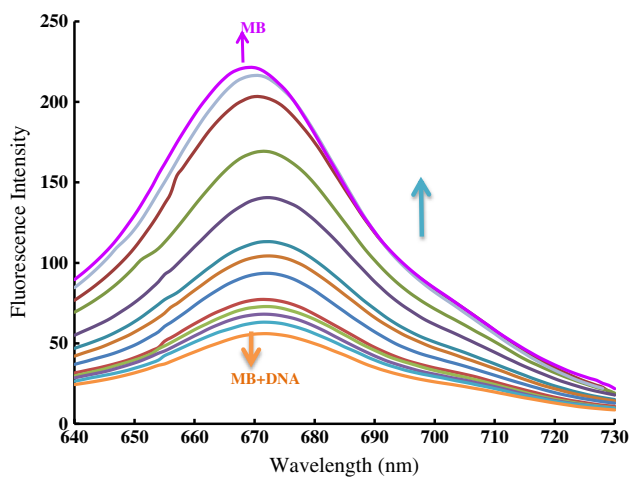


Figure 8. Emission spectra of the MB–DNA complexes on adding various concentration of EFZ, $c(\text{MB}) = 5 \times 10^{-6} \text{ mol L}^{-1}$, $c(\text{DNA}) = 5 \times 10^{-5} \text{ mol L}^{-1}$, $c(\text{EFZ}) (\times 10^5 \text{ mol L}^{-1})$: 0.00, 1.00, 1.90, 2.85, 3.80, 4.70, 6.90, 8.95, 10.00, 12.80, 16.10, 19.00, $\lambda_{\text{ex}} = 630 \text{ nm}$ at 310 K.

of the DNA–MB complex increased with increasing concentrations of EFZ. When EFZ was added directly into the MB solution, the change of MB fluorescence intensity was not observed. This finding indicates that EFZ does not react with MB when DNA is absent. The increase in the fluorescence intensity could be due to a greater amount of free MB molecules; in other words, the MB molecules were released after the addition of EFZ and the fluorescence of the solution was increased. Therefore, the formation of EFZ–DNA prevents the binding of MB. Consequently, recovery of MB fluorescence is indicative of an intercalative mode of binding; this experiment confirms our previous evidence.

Iodide quenching studies

Further support for the intercalative binding of efavirenz to DNA was obtained through iodide quenching experiments. It is well known that intercalation of small molecules into DNA double helix stands protects the entrapped molecules from an ionic quencher and consequently, fluorescence quenching of the probe by an ionic quencher is not expected in an intercalated condition (32). By contrast, in electrostatic binding and groove binding, the probe molecules are exposed to the quencher in the aqueous phase, and the fluorescence of the probe molecule should be quenched efficiently (33). Negatively charged I^- was selected for this purpose. In aqueous solutions, potassium iodide quench the fluorescence of EFV very efficiently, so we used the anionic quencher to determine the relative accessibilities of the free and bound EFV. The quenching constants (KSV) were obtained from Stern–Volmer equation. The values of KSV of EFZ by I^- ion in the absence and presence of DNA were calculated to be 541.9 and 389.5 L mol^{-1} , respectively. (shown in Fig. 9).

The decreases of the quenching constants of KI on EFZ after adding DNA resulted from the intercalative binding of EFZ with the DNA double helix, which prevented fluorescence quenching of EFZ from anionic quenchers because of the sandwich structure formed by EFZ and two DNA base pairs as well as by the polyphosphate anionic skeleton of DNA.

Circular dichroism spectroscopy

Circular dichroic spectroscopic techniques give us useful information on how the conformation of DNA is influenced by the binding of the drug to DNA. The changes in CD signals of DNA observed on interaction with drugs may often be assigned to the corresponding changes in DNA structure. The observed CD spectrum of calf

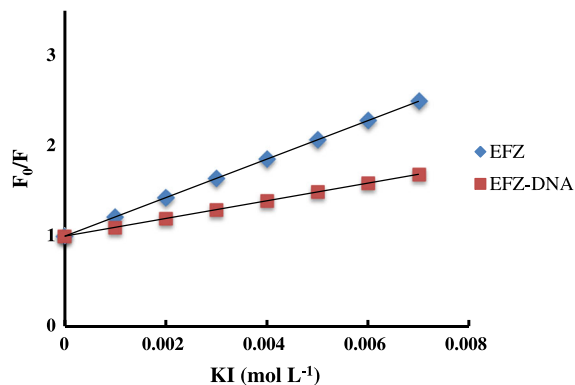


Figure 9. Fluorescence quenching plots of [EFZ] by KI in the absence and presence of DNA. $[\text{EFZ}] = 5 \times 10^{-5} \text{ mol L}^{-1}$; $[\text{DNA}] = 2.5 \times 10^{-4} \text{ mol L}^{-1}$.

thymus DNA consists of a positive band at 275 nm due to base stacking and a negative band at 245 nm due to helicity, which is characteristic of DNA in the right-handed B form (6,38). Simple groove binding and electrostatic interaction of small molecules with DNA show less or no perturbations on the base stacking and helicity bands, while binding via the intercalation mode in classic intercalators such as MB, causes change in intensities of both the bands and stabilizing the right-handed B conformation of CT-DNA (39). The effect of EFZ on the conformation of the secondary structure of DNA was studied by keeping the concentration of CT-DNA at $5.0 \times 10^{-5} \text{ mol L}^{-1}$, while varying the concentration of EFZ. The results of CD studies indicated that when the [EFZ]/[DNA] ratio was increased, clear changes occurred in the CD spectra. In Fig. 10, the changes in the CD spectrum of CT-DNA in the presence

of increasing concentrations of EFZ were depicted. The intensities of negative bands decreased along with a bathochromic effect about 3.0 nm, while the positive bands increased. The positive band showed increase in molar ellipticity without any significant shift in the band maxima when the EFZ concentration was increased progressively.

The changes in the CD spectra may reflect a shift from a B-like DNA structure toward one with some contributions from an A-like conformation (40–42). It has been reported that an enhancement of the CD band of DNA at 275 nm is due to distortions induced in the DNA structure (6). In addition, a red shift in the CD spectra at 245 nm suggested that interactions exist between the aromatic ring of the drug and the DNA base pairs (43). Therefore, we think that the increase in CD signals around 275 nm, along with increasing the EFZ concentration, is important evidence for the intercalation of this anti-viral drug with the DNA base pairs, which concurs with other previously reported data (34,43).

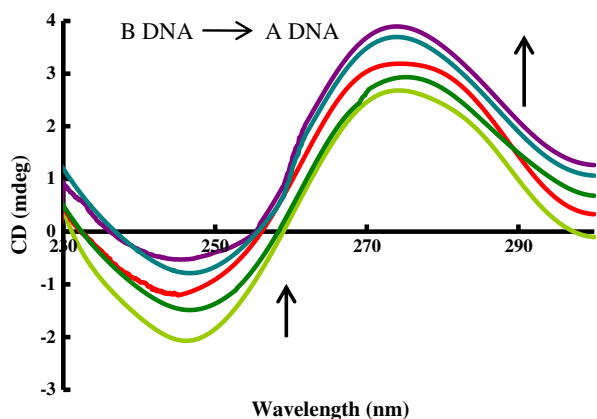


Figure 10. Changes in the CD spectra of $5.0 \times 10^{-5} \text{ mol L}^{-1}$ DNA in the absence and presence of EFZ; c (EFZ) ($\times 10^3 \text{ mol L}^{-1}$): 0.00, 1.50, 3.50, 6.50, 7.50 and 298 K.

Binding region

According to the above discussion, the binding mechanism between EFZ and DNA is an intercalation. The influences of DNA bases, C, G, A and T on the UV/vis absorption spectra of EFZ were used to confirm the binding region of EFZ. Figure 11 reveals the changes in the UV/vis absorption spectra after the addition of different bases to a EFZ solution. The absorption intensity enhanced gradually with the increase in the four types of bases. As shown in Fig. 8, in the vicinity of 250 nm, the binding force of EFZ with C and G is greater than that with A and T. The results suggested that EFZ could interact with the four types of bases, however, the interactive forces of EFZ with C and G were greater than with A and T, and EFZ bound mainly to C–G enriched regions of the DNA, that is intercalative binding.

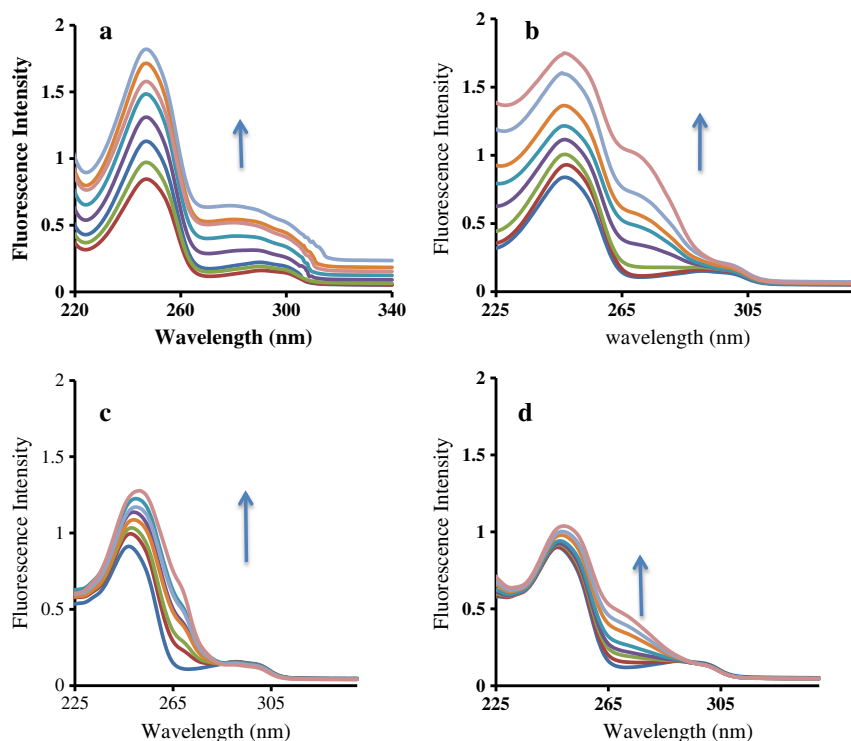


Figure 11. UV/vis absorption spectra of EFZ after adding different concentrations of G (a); A (b); T (c); and C (d). [EFZ] = $5.0 \times 10^{-5} \text{ mol L}^{-1}$; [G] = 0.05 mol L^{-1} , [C] = 0.05 mol L^{-1} , [A] = 0.05 mol L^{-1} , [T] = 0.05 mol L^{-1} (1 μL per scan; 0–8 μL).

Viscosity studies

Optical photophysical probes generally provide necessary, but not sufficient, clues to support binding mode. Hydrodynamic measurements that are sensitive to length change (i.e. viscosity and sedimentation) are regarded as the least ambiguous and the most critical tests of binding in solution in the absence of crystallographic structural data. A classical intercalative mode causes a significant increase in viscosity of DNA due to an increase in separation of base pairs at intercalation sites and hence an increase in overall DNA length occurs. In contrast, a partial, non-classical intercalation of molecule could bend or kink the DNA helix, reducing its length and, concomitantly, its viscosity (44,45).

In addition, molecules that bind exclusively in the DNA grooves by partial and/or non-classical intercalation, under the same conditions, typically cause less pronounced (positive or negative) or no change in DNA solution viscosity (6,46). The values of relative specific viscosity $(\eta/\eta_0)^{1/3}$ versus $([EFZ]/[DNA])$, in the absence and in the presence of EFZ were plotted (Fig. 12). It can be observed that the viscosity of the DNA increases steadily with increasing amounts of EFZ. Such behavior is accordance with other intercalators, and increases the relative specific viscosity for lengthening of the DNA double helix, resulting from intercalation. These results indicate that EFZ can intercalate into the adjacent DNA base pairs, causing an extension in the helix and thus increase the viscosity of DNA (6,12).

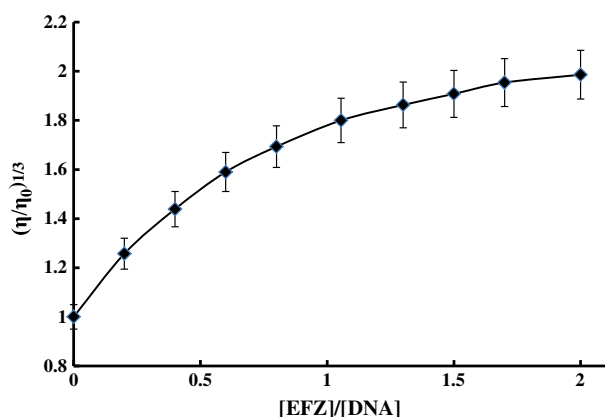


Figure 12. Effect of increasing amounts of EFZ on the viscosity of DNA, c (DNA) = $5.0 \times 10^{-5} \text{ mol L}^{-1}$ in $5.0 \times 10^{-2} \text{ mol L}^{-1}$ HEPES buffer, c (EFZ) ($\times 10^5 \text{ mol L}^{-1}$): 0.00, 1.00, 2.00, 3.00, 5.00, 6.50, 7.50, 8.50, 10.00).

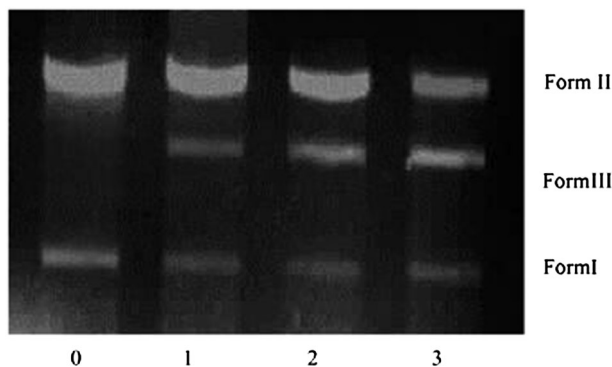


Figure 13. Gel electrophoresis of pUC18 ($5.0 \times 10^{-4} \text{ mol L}^{-1}$) in the presence of increasing amounts of EFZ ($[EFZ]/[DNA] = 0.0, 0.5, 1.0, 1.5$).

Gel electrophoresis

The cleavage of plasmid DNA can be seen by agarose-gel electrophoresis. When circular plasmid DNA is subject to electrophoresis, relatively fast migration is commonly observed for the intact supercoiled Form I. When scission occurs on one strand (nicking), the supercoil relaxes to form a slower moving, open-circular Form II. When both strands are intercepted, a linear Form III is generated that migrates between Form I and Form II DNA (47). In order to assess any devastation of the DNA as a result of binding, EFZ agarose-gel electrophoresis has been performed with the circular form of plasmid DNA. Figure 13 shows gel electrophoresis separation of pUC18 DNA after incubation with EFZ, as well as showing the migration of conversion of Forms I–III after 60 min irradiation in the presence of varying concentrations of EFZ. With increasing concentration of EFZ, the amount of Form I DNA diminishes gradually, whereas that of Form II increases. Line 0 has DNA alone as control line. In lane 4 Form II of plasmid DNA was converted to

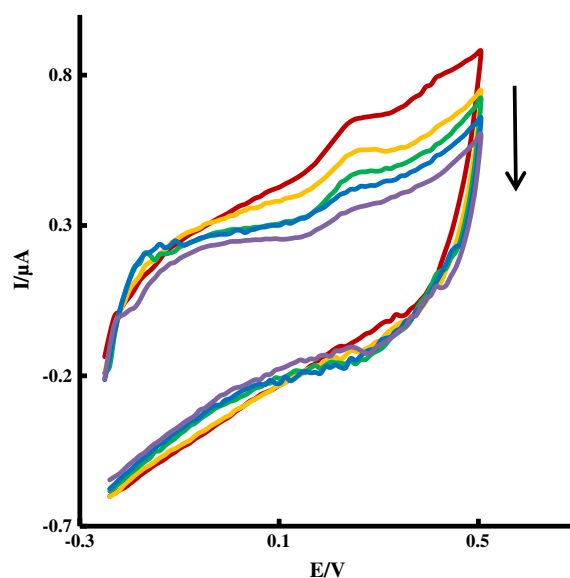


Figure 14. Cyclic voltammogram of $2.0 \times 10^{-5} \text{ mol L}^{-1}$ EFZ on a polished glassy carbon electrode in the absence and presence of different concentrations of DNA.

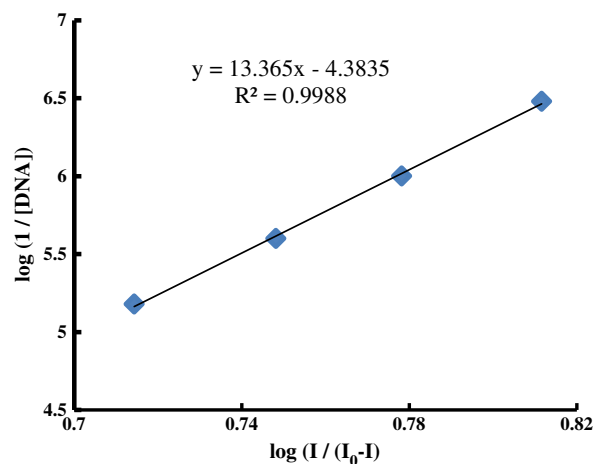


Figure 15. Plot of $\log(1/[DNA])$ versus $\log(I/(I_0 - I))$ for 0.5 m mol L^{-1} EFZ with varying concentrations of DNA used to calculate the binding constant of the EFZ–DNA adduct.

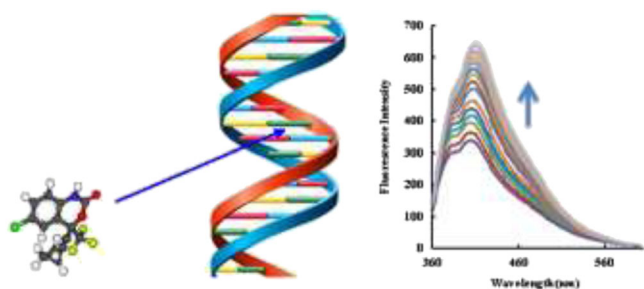


Figure 16. Fluorescence spectra of the EFZ ($5 \times 10^{-5} \text{ mol}^{-1} \text{ L}$) in the absence and presence of increasing amounts of DNA ($[\text{DNA}] / [\text{EFZ}] = 0.00, .0.10, 0.30, 0.45, 0.55, 0.65, 0.80, 1.00, 1.25, 1.35, 1.60, 1.85, 2.00, 2.35, 2.75, 3.00$) and 310 K.

Form III, indicating two subsequent and nearby non-random single-stranded breaks in DNA.

Cyclic voltammetry

The application of an electrochemical technique to study the interaction of electroactive compounds with DNA provided a useful complement to the optical techniques. In the present study this technique was employed to understand the nature of DNA binding to EFZ and the results are shown in Fig. 14. As shown in this figure, EFZ presents a well defined oxidation peak at about 0.25 V. This anodic peak can be attributed to the oxidation of the nitrogen atom on the benzoxazine ring (48). In the presence of DNA, the cyclic voltammograms of EFZ exhibited positive shift in the anodic peak potential followed by a decrease in the peak current, indicating the interaction that exists between EFZ and DNA. The decreases in peak current can be explained in terms of slow diffusion of EFZ bound to the large DNA molecules (49), and also support the changes found in CV experiments. Hence it can be concluded that the EFZ molecule binds to DNA via intercalation, with insertion of the EFZ molecule between the base pairs of the DNA duplex strand.

The interaction of EFZ with DNA can be described using eqn (9):



The binding constant, K , of the interaction of EFZ with DNA was determined according to the following equation (50):

$$\log\left(\frac{1}{[\text{DNA}]}\right) = \log(K) + \log\left(\frac{I_{\text{Free}}}{I_{\text{Free}} - I_{\text{Bond}}}\right) \quad (10)$$

where K is the apparent binding constant, I_{Free} and I_{Bond} the peak current of the free guest and the adduct, respectively. The plot of $\log(1/[\text{DNA}])$ versus $\log(I_{\text{Free}}/(I_{\text{Free}} - I_{\text{bond}}))$ (Fig. 15) becomes linear with the intercept of $\log(K)$ according to (eqn (10)). Binding constants of EFZ and DNA were calculated to be $2.40 \pm 0.04 \times 10^4 \text{ mol}^{-1} \text{ L}$ using CV data (eqn (10)), which is very similar to that calculated using spectrophotometry data (Table 2).

Conclusion

We have explored the binding interaction of EFZ with CT-DNA in physiological buffer using multispectroscopic techniques, cyclic voltammetry viscosity measurement, and gel electrophoresis. The binding constants of this complex with DNA were measured at different temperatures, and the thermodynamic parameters were calculated. It was found that hydrogen bonds and van der Waals

forces play a major role in the binding of EFZ to DNA. The intrinsic binding constant observed ($K_b = 3.50 \pm 0.06 \times 10^4 \text{ mol}^{-1} \text{ L}$) was roughly comparable to other intercalators.

The intercalative binding of the drug with DNA (Fig. 16) was deduced by taking account of relevant UV-vis absorption spectra, circular dichroism, fluorescence spectra, iodide quenching effect, cyclic voltammetry and viscosity measurements. CD results showed deep conformational changes in the CT-DNA double helix upon binding with the drug. The increase in the relative viscosity as well as melting temperature ($5\text{--}6^\circ\text{C}$) of CT-DNA in the presence of EFZ showed that intercalation must be the predominant form of binding. Also, it was shown that this complex could induce DNA cleavage. This study is expected to provide greater insight into the use of anti-viral drugs as anti-cancer agents.

Acknowledgements

The authors gratefully acknowledge the support of this work by Razi University Research Council.

References

- Riahi S, Eynollahi S, Ganjali MR, Norouzi P. Computational studies on effects of efavirenz as an anticancer drug on DNA: application in drug design. *Int J Electrochem Sci* 2010;5:815–827.
- Haas DW, Fessel WJ, Delapenha RA, Manion DJ. Therapy with efavirenz plus indinavir in patients with extensive prior nucleoside reverse-transcriptase inhibitor experience: a randomized, double-blind, placebo-controlled trial. *J Infect Dis* 2001;183:392–400.
- Marzolini C, Telenti A, Buclin T, Biollaz A. Simultaneous determination of the HIV protease inhibitors indinavir, amprenavir, saquinavir, ritonavir, nelfinavir and the non-nucleoside reverse-transcriptase inhibitor efavirenz by high performance liquid chromatography after solid phase extraction. *J Chromatogr B Biomed Sci Appl* 2000;740:43–58.
- Ni YN, Wei M, Kokot S. Electrochemical and spectroscopic study on the interaction between isoprenaline and DNA using multivariate curve resolution-alternating least squares. *Int J Biol Macromol* 2011;49:622–8.
- Goodwin KD, Lewis MA, Tanious FA, Tidwell RR, Wilson WD, Georgiadis MM, *et al.* A high-throughput, high-resolution strategy for the study of site-selective DNA-binding agents: analysis of a 'highly twisted' benzimidazole-diamidine. *J Am Chem Soc* 2006;128:7846–54.
- Shahabadi N, Kashanian S, Darabi F. *In vitro* study of DNA interaction with a water-soluble dinitrogen Schiff base. *DNA Cell Biol* 2009;28:589–96.
- Song Y, Zhong D, Luo J, Tan H, Chen S, Li P, *et al.* Binding characteristics and interactive region of 2-phenylpyrazolo[1,5-c]quinazoline with DNA. *Luminescence* 2014;29:1141–7.
- Erkkila KE, Odom RT, Barton JK. Recognition and reaction of metallointercalators with DNA. *Chem Rev* 1999;99:2777–96.
- Lerman LS. Structural considerations in the interaction of DNA and acridines. *J Mol Biol* 1961;3:18–30.
- Shahabadi N, Maghsudi M, Mahdavi M, Pourfoulad M. Interaction of calf thymus DNA with the antiviral drug lamivudine. *DNA Cell Biol* 2012;31:122–7.
- Shahabadi N, Mirzaei Kalar Z, Hosseinpour MN. DNA interaction studies of a platinum (II) complex containing an anti-viral drug, ribavirin: the effect of metal on DNA binding. *Spectrochim Acta A* 2012;96:723–8.
- Shahabadi N, Fatahi N, Mahdavi M, Kiani Nejad Z, Pourfoulad M. Multispectroscopic studies of the interaction of calf thymus DNA with the anti-viral drug, valacyclovir. *Spectrochim Acta A* 2011;83:420–4.
- Ahmadi F, Alizadeh AA, Shahabadi N, Rahimi-Nasrabadi M. Study binding of Al-curcumin complex to ds-DNA, monitoring by multispectroscopic and voltammetric techniques. *Spectrochim Acta A* 2011;79:1466–74.
- Uno T, Hamasaki K, Tanigawa M, Shimabayashi S. Binding of meso-tetrakis(*N*-methylpyridinium-4-yl)porphyrin to double helical RNA and DNA.RNA hybrids. *Inorg Chem* 1997;36:1676–83.
- Grueso E, López-Pérez G, Castellano M, Prado-Gotor R. Thermodynamic and structural study of phenanthroline derivative ruthenium

- complex/DNA interactions: probing partial intercalation and binding properties. *J Inorg Biochem* 2012;106:1–9.
16. Kashanian S, Shahabadi N, Roshanfekr H, Shalmashi K, Omidfar K. DNA-binding studies of PdCl₂ (LL) (LL chelating diamine ligand: *N,N*-dimethyltrimethylenediamine) complex. *Biochemistry (Moscow)* 2008;73:929–36.
 17. Shahabadi N, Kashanian S, Purfoulad M. DNA interaction studies of a platinum(II) complex, PtCl₂(NN)(NN,4,7-dimethyl-1,10-phenanthroline), using different instrumental methods. *Spectrochim Acta A* 2009;72: 757–61.
 18. Jayamani A, Thamilarasan V, Sengottuvelan N, Manisankar P, Kang SK, Kim YI, *et al.* Synthesis of mononuclear copper(II) complexes of acyclic Schiff's base ligands: spectral, structural, electrochemical, antibacterial, DNA-binding and cleavage activity. *Spectrochim Acta A* 2014;122: 365–74.
 19. Kashanian S, Khodaei MM, Roshanfekr H, Shahabadi N, Mansouri G. DNA binding, DNA cleavage and cytotoxicity studies of a new water soluble copper(II) complex: The effect of ligand shape on the mode of binding. *Spectrochim Acta A* 2012;86:351–9.
 20. Bahr M, Gabelica V, Granzhan A, Teulade-Fichou MP, Weinhold E. Selective recognition of pyrimidine–pyrimidine DNA mismatches by distance-constrained macrocyclic bis-intercalators. *Nucleic Acids Res* 2008;36:5000–12.
 21. Bischoff G, Hoffman S. DNA-binding of drugs used in medicinal therapies. *Curr Med Chem* 2002;9:321–348.
 22. Hu Z, Tong CL. Synchronous fluorescence determination of DNA based on the interaction between methylene blue and DNA. *Anal Chim Acta* 2007;587:187–93.
 23. Liu ZQ, Li YT, Wu ZY, Song YL. A two-dimensional copper (II) polymer with bridging μ -trans-oxamidate and μ^2 -picrate ligands: synthesis, crystal structure and DNA binding studies. *Inorg Chim Acta* 2008;361:226–32.
 24. Barton JK, Goldberg JM, Kumar CV, Turro NJ. Binding modes and base specificity of tris(phenanthroline)-ruthenium(II) enantiomers with nucleic acids: tuning the stereoselectivity. *J Am Chem Soc* 1986;108:2081–8.
 25. Wang BD, Yang ZY, Wang Q, Cai TK, Crewdson P. Synthesis, characterization, cytotoxic activities, and DNA-binding properties of the La(III) complex with naringenin Schiff-base. *Bioorg Med Chem* 2006;14: 1880–8.
 26. Shahabadi N, Fatahi A. multispectroscopic DNA-binding studies of a Tris-chelate nickel(II) complex containing 4,7-diphenyl 10-phenanthroline ligands. *J Mol Struct* 2010;970:90–5.
 27. Wilson DW, Jones RL. Intercalating drugs: DNA binding and molecular pharmacology. *Adv Pharmacol Chemother* 1981;18: 177–196.
 28. Song G, Yan Q, He Y. Studies on interaction of norfloxacin, Cu²⁺, and DNA by spectral methods. *J Fluoresc* 2005;15:673–8.
 29. Wilson WD, Tanious FA, Barton HJ, Jones RL, Strekowski L, Boykin DW. Binding of 4,6-diamidino-2-phenylindole(DAPI) to GC and mixed sequences in DNA: intercalation of a classical groove-binding molecule. *J Am Chem Soc* 1989;111:5008–10.
 30. Ross DP, Subramanian S. Thermodynamics of protein association reactions: forces contributing to stability. *J Biochem* 1981;20: 3096–3102.
 31. Nike DB, Moorthy PN, Priyadarsini KI. Nonradiative energy transfer from 7-amino coumarin dyes to thiazine dyes in methanolic solutions. *Chem Phys Lett* 1990;168:533–8.
 32. Liu HK, Sadler PJ. Metal complexes as DNA intercalators. *Acc Chem Res* 2011;44:349–359.
 33. Zimmerman F, Hossenfelder B, Panitz JC, Wokaun A. SERRS study of acridine orange and its binding to DNA strands. *J Phys Chem* 1994;98:12796–12804.
 34. Kashanian S, Askari S, Ahmadi F, Omidfar K, Ghobadi S, Abbasi TF. In vitro study of DNA interaction with clodinafop-propargyl herbicide. *DNA Cell Biol* 2008;27:581–6.
 35. Tuite E, Norden B. Sequence-specific interactions of ethylene-blue with polynucleotides and DNA—a spectroscopic study. *J Am Chem Soc* 1994;116:7548–56.
 36. Fujimoto BS, Clendenning JB, Delrow JJ, Heath PJ, Schurr M. Fluorescence and photobleaching studies of methylene blue binding to DNA. *J Phys Chem* 1994;98:6633–43.
 37. Long EC, Barton JK. On demonstrating and intercalation. *Acc Chem Res* 1990;23:271–3.
 38. Ivanov VI, Minchenkova LE, Schyolkina AK, Polytayev AI. Different conformations of double-stranded nucleic acid in solution as revealed by circular dichroism. *Biopolymers* 1973;12:89–110.
 39. Collins JG, Tp S, Barton JK. ¹H-NMR of Rh(NH₃)₄phi³⁺ bound to d (TGGCCA)₂: classical intercalation by a nonclassical octahedral metallointercalator. *J Am Chem Soc* 1994;116:9840–6.
 40. Poklar N, Pilch DS, Lippard SJ, Redding EA, Dunham SH, Breslauer KJ. Influence of cisplatin intrastrand crosslinking on the conformation, thermal stability, and energetics of a 20-mer DNA duplex. *Proc Natl Acad Sci U S A* 1996;93:7607–11.
 41. Li FH, Zhao GH, Wu HX, Lin H, Wu XX, Zhu SR, *et al.* Synthesis, characterization and biological activity of lanthanum(III) complexes containing 2-methylene-1,10-phenanthroline units bridged by aliphatic diamines. *J Inorg Biochem* 2006;100:36–43.
 42. Shahabadi N, Maghsudi M. Gel electrophoresis and DNA interaction studies of the food colorant quinoline yellow. *Dyes Pigments* 2013;96:377–82.
 43. Zhong W, Yu J, Liang Y, Fan K, Lai L. Chlorobenzylidene-calf thymus DNA interaction II: Circular dichroism and nuclear magnetic resonance studies. *Spectrochim Acta A* 2004;60:2985–92.
 44. Satyanarayana S, Dabrowiak JC, Chaires JB. Neither Δ- nor Λ-tris(phenanthroline)ruthenium (III) binds to DNA by classical intercalation. *Biochemistry* 1992;31:9319–24.
 45. Zou XH, Ye BH, Li H, Liu JG, Xiong Y, Ji LN. Mono and binuclear ruthenium(II) complexes containing a new asymmetric ligand 3-(pyrazin-2-yl)-as-triazino[5,6-f]1,10-phenanthroline: synthesis, characterization and DNA-binding properties. *J Chem Soc Dalton Trans* 1999;9:1423–8.
 46. Huang HL, Liu YJ, Zeng CH, He LX, Wu FH. In vitro cytotoxicity, apoptosis, DNA-binding, and antioxidant activity studies of ruthenium (II) complexes. *DNA Cell Biol* 2010;29:261–70.
 47. Arjmand F, Sayeed F, Muddassir M. Synthesis of new chiral heterocyclic Schiff base modulated Cu (II)/Zn (II) complexes: their comparative binding studies with CT-DNA, mononucleotides and cleavage activity. *J Photochem Photobiol B* 2011;103:166–79.
 48. Topal BD, Uslu B, Ozkan SA. Voltammetric studies on the HIV-1 inhibitory drug efavirenz: the interaction between dsDNA and drug using electrochemical DNA biosensor and adsorptive stripping voltammetric determination on disposable pencil graphite electrode. *Biosens Bioelectron* 2009;24:2358–64.
 49. Fei Y, Lu G, Fan G, Wu Y. Spectroscopic studies on the binding of a new quinolone antibacterial agent: sinifloxacin to DNA. *Anal Sci* 2009;25:1333–8.
 50. Feng Q, Li NQ, Jiang YY. Electrochemical studies of porphyrin interacting with DNA and determination of DNA. *Anal Chim Acta* 1997;344:97–104.